Published in final edited form as:
Mol Cancer Ther. 2010 April ; 9(4): 1019–1027. doi:10.1158/1535-7163.MCT-09-0862.

Pretargeted ImmunoPET Imaging of CEA-expressing Tumors with a Bispecific Antibody and a ^{68}Ga- and ^{18}F-labeled Hapten-peptide in Mice with Human Tumor Xenografts

Rafke Schoffelen[1], **Robert M. Sharkey**[2], **David M. Goldenberg**[2], **Gerben Franssen**[1], **William J. McBride**[3], **Edmund A. Rossi**[4], **Chien-Hsing Chang**[3,4], **Peter Laverman**[1], **Jonathan A. Disselhorst**[1], **Annemarie Eek**[1], **Winette T.A. van der Graaf**[5], **Wim J.G. Oyen**[1], and **Otto C. Boerman**[1]

[1] Department of Nuclear Medicine, Radboud University Nijmegen Medical Centre, Nijmegen, The Netherlands [2] Garden State Cancer Center, Center for Molecular Medicine and Immunology, Belleville, NJ 07109, USA [3] IBC Pharmaceuticals, Inc., Morris Plains, NJ 07950, USA [4] Immunomedics, Inc., Morris Plains, NJ 07950, USA [5] Department of Medical Oncology, Radboud University Nijmegen Medical Centre, Nijmegen, The Netherlands

Abstract

^{18}F-Fluorodeoxyglucose (^{18}F-FDG) is the most common molecular imaging agent in oncology, with a high sensitivity and specificity for detecting a number of cancers. Antibodies could enhance specificity; therefore, procedures were developed for radiolabeling a small (~1.5 kD) hapten-peptide with ^{68}Ga or ^{18}F to compare their specificity to ^{18}F-FDG for detecting tumors using a pretargeting procedure. Mice were implanted with carcinoembryonic (CEA; CEACAM5)-expressing LS174T human colonic tumors, a CEA-negative tumor, or an inflammation was induced in thigh muscle. A bispecific monoclonal (bsMAb) anti-CEA × anti-hapten antibody was given to mice, and 16 h later, 5 MBq of ^{68}Ga- or ^{18}F-labeled hapten-peptides were administered intravenously. Within 1 h, tissues showed high and specific targeting of the ^{68}Ga-IMP-288, with 10.7 ± 3.6% ID/g uptake in the tumor and very low uptake in normal tissues (e.g., tumor/blood 69.9 ± 32.3), in a CEA-negative tumor (0.35 ± 0.35% ID/g), and inflamed muscle (0.72 ± 0.20% ID/g). ^{18}F-FDG localized efficiently in the tumor (7.42 ± 0.20% ID/g), but also in the inflamed muscle (4.07 ± 1.13% ID/g) and in a number of normal tissues; thus, pretargeted ^{68}Ga-IMP-288 provided better specificity and sensitivity. PET/CT images reinforced the improved specificity of the pretargeting method. ^{18}F-labeled IMP-449 distributed similarly in the tumor and normal tissues as the ^{68}Ga-labeled IMP-288, indicating that either radiolabeled hapten-peptide could be used. Thus, pretargeted immunoPET performs exceptionally well with short-lived radionuclides, and is a highly sensitive procedure that is more specific than ^{18}F-FDG-PET.

Keywords

PET; pretargeting; bispecific antibody; gallium-68; fluorine-18; colorectal neoplasms; mice

Request for reprints: Rafke Schoffelen, Radboud University Nijmegen Medical Centre, Department of Nuclear Medicine, PO Box 9101, 6500 HB Nijmegen, The Netherlands. Phone: +31-24-3619097 ; Fax: +31-24-3618942; r.schoffelen@nucmed.umcn.nl.

Disclosure of Potential Conflicts of Interest: W.J. McBride, D.M. Goldenberg, E.A. Rossi, and C-H. Chang are employed by or have financial interest in Immunomedics, Inc., and/or IBC Pharmacauticals, Inc.; the other authors disclosed no potential conflicts of interest.

Introduction

Radiolabeled antibody targeting of tumor-associated antigens often requires several days for adequate visualization of tumors due to the slow pharmacokinetics and accretion of intact antibodies in tumors (1). The use of antibody fragments and engineered antibody formats (such as $F(ab')_2$, Fab′, diabodies, minibodies or scFv) has improved radioimmunodetection only to a limited extent. Tumor uptake of most antibody fragments is much lower than that of an IgG, resulting in reduced signal strength in the tumors, which can contribute to uncertainties in interpretation (2). Pretargeting techniques were developed to improve radioimmunotargeting of tumors (3-5). In pretargeting, an unlabeled bifunctional reagent with affinity for the tumor and a small radiolabeled molecule is given in advance of the radiolabeled compound (4-6). Two main antibody-based pretargeting approaches can be distinguished: strategies that use (strept)avidin and biotin, and those that use bispecific monoclonal antibodies (bsMAb). The disadvantages of the biotin-avidin-based approaches are the immunogenicity of (strept)avidin and the need for a clearing agent to remove the antibody conjugate from the blood (4). A bsMAb, which can be humanized to reduce immunogenicity, will bind a tumor-associated antigen and a hapten. Coupling 2 haptens together improves peptide uptake and stability by a process known as affinity enhancement (7). Chelate-metal complexes, such as DTPA-In, have been used as haptens (8). More recently, peptides substituted with the hapten, histamine-succinyl-glycine (HSG), in combination with anti-HSG bsMAbs have provided a more flexible system, because these HSG-substituted peptides can be conjugated with various chelating moieties (DTPA, DOTA, N_3S-chelates, etc.). As a result they can be labeled with a wide variety of radionuclides, like ^{111}In and ^{99m}Tc for SPECT imaging (6), with ^{124}I for PET imaging (9, 10), or with ^{131}I, ^{90}Y and ^{177}Lu for pretargeted radioimmunotherapy (11).

Previous studies illustrated the enhanced sensitivity of pretargeted imaging for detecting cancer (6,10,12), with superior results of pretargeting compared to the directly radiolabeled antibody fragment. In a micrometastatic human colon cancer model, tumor nodules no larger than 0.3 mm in diameter were detected in the lungs of athymic mice with the ^{124}I-labeled di-HSG-peptide (12). This study highlighted the exceptional sensitivity of the pretargeting procedure, but herein we also wanted to examine the specificity of pretargeting, and therefore included a model of sterile inflammation.

Earlier studies were performed with ^{124}I because it was commercially available and the chemistry for iodination was well known. However, ^{124}I is not an ideal radionuclide for PET imaging due to its high-energy positrons and considerable expense. Its long half-life ($t_{½}$ = 4.2 days) has been an advantage for directly radiolabeled antibodies that require extended periods for adequate contrast to develop, which only takes 1 h with pretargeting, making this method more amenable to short-lived positron emitting radionuclides. There are currently two radionuclides with exceptional imaging properties for PET, namely ^{68}Ga and ^{18}F, and their half-lives are well matched with the pharmacokinetics of the radiolabeled peptide (^{68}Ga $t_{½}$ = 68 min; and ^{18}F, $t_{½}$ = 110 min). ^{68}Ga is a relative newcomer to nuclear medicine, and in addition to its physical properties, it is readily available in a nearly carrier-free state from an in-house ^{68}Ge/^{68}Ga generator.

Herein we report the first pretargeting studies with this ^{68}Ga-labeled peptide. ^{18}F has been the gold standard for PET studies. It is abundantly available and inexpensive, but the chemistry involved in preparing labeled products can be challenging. We recently reported a simplified approach for preparing ^{18}F-labeled peptides that involves the formation of ^{18}F-aluminum complexes that can then be simply bound to a chelate on a peptide (13). Thus, another objective of this study was to compare a ^{68}Ga- and an ^{18}F-labeled peptide with pretargeting.

In summary, we show the feasibility of using ^{68}Ga- or ^{18}F-labeled di-HSG-peptides in pretargeting, and further demonstrate the improved specificity afforded by pretargeting by including a comparison of ^{18}F-FDG and an inflammation model.

Materials and Methods

Pretargeting reagents TF2, IMP-288 and IMP-449

The bsMAb, TF2, and the peptides IMP-288 and IMP-449, were provided by Immunomedics (Morris Plains, NJ, USA). TF2 is an engineered trivalent bispecific antibody composed of a humanized anti-histamine-succinyl-glycine (HSG) Fab-fragment derived from the 679 anti-HSG monoclonal antibody (14), and two humanized anti-CEA Fab-fragments derived from the hMN-14 antibody or labetuzumab (14,15), formed into a 157 kD protein by the Dock-and-Lock procedure (16,17). The immunoreactive fraction of TF2 for binding to CEA, determined in a Lindmo assay (18) on fixed LS174T cells, exceeded 85%. Gel fitration chromatography showed that TF2 could bind >90% of ^{68}Ga-IMP-288 peptide.

IMP-288 was synthesized and purified as described by McBride et al. (10). It is a DOTA-conjugated D-Tyr-D-Lys-D-Glu-D-Lys tetrapeptide in which both lysine residues are substituted with a HSG-moiety via their ε-aminogroup: 7,10-tetra-azacyclododecane-N,N′,N″,N‴-tetraacetic acid (DOTA)-D-Tyr-D-Lys(HSG)-D-Glu-D-Lys(HSG)-NH_2 (Figure 1a). A similar peptide, IMP-449, was conjugated with 1,4,7-tri-azacyclononane-N,N′,N″-triacetic acid (NOTA) instead of DOTA, to facilitate labeling with ^{18}F (Figure 1b). To improve the conjugation of the NOTA chelator an alanine residue was used as a spacer (13).

TF2 was labeled with ^{125}I (Perkin Elmer, Waltham, MA) by the iodogen method (19), to a specific activity of 58 MBq/nmol. ^{125}I-labeled TF2 was purified by eluting the reaction mixture with PBS, 0.5 % *w/v* bovine serum albumin (BSA) (Sigma Chemicals, St. Louis, MO, USA) on a PD-10 column (GE Healthcare Bio-Sciences AB, Uppsala, Sweden).

Labeling of IMP-288 or IMP-449

IMP-288 was labeled with ^{111}In (Covidien, Petten, The Netherlands) at 32 MBq/nmol under strict metal-free conditions. Briefly, 11 MBq ^{111}In was added to 12 μg IMP-288 in 0.25 M ammonium acetate (NH_4Ac) buffer, pH 5.6, and after 20 min at 95 °C, 10 μL 50 mM ethylenediaminetetraacetic acid (EDTA) was added to complex any unbound ^{111}In.

IMP-288 was labeled with ^{68}Ga eluted from a TiO-based 1,110 MBq ^{68}Ge/^{68}Ga generator (Cyclotron Co. Ltd., Obninsk, Russia) using 0.1 M ultrapure HCl (J.T. Baker, Deventer, The Netherlands). Five, 1-ml fractions were collected and the second fraction was used for labeling the peptide. One volume of 1.0 M HEPES buffer, pH 7.0, was added to 3.4 nmole IMP-288. Four volumes of ^{68}Ga eluate (380 MBq) were added and the mixture was heated at 95 °C for 20 min. EDTA (50 mM) was added to a final concentration of 5 mM to complex the non-chelated $^{68}Ga^{3+}$, followed by purification on a 1-mL Oasis HLB-cartridge (Waters, Milford, MA). After washing the cartridge with water, the peptide was eluted with 25% ethanol.

IMP-449 was labeled with ^{18}F as described by McBride et al. (13). [^{18}F]Fluoride (555-740 MBq; B.V. Cyclotron VU, Amsterdam, The Netherlands) was eluted from a QMA cartridge with 0.4 M $KHCO_3$. Four 200-μL fractions were collected in vials containing 3 μL 2 mM $AlCl_3$ in 0.1 M sodium acetate buffer, pH 4. The fraction with highest activity was used. The $Al[^{18}F]^{2+}$ activity was added to a vial containing IMP-449 (230 μg) and ascorbic acid (10 mg). The mixture was incubated at 100 °C for 15 min, then purified by reversed phase-high performance liquid chromatography (RP-HPLC; Phenomenex Onyx monolithic C18 column, Torrance, CA), using a linear gradient of 97% A to 100% B in 30 min (Buffer A: 0.1% TFA in water; Buffer B: 0.1% TFA in acetonitrile, flow rate: 3 mL/min). After adding one volume

of water, the peptide was purified on a 1-mL Oasis HLB cartridge. After washing with water, the radiolabeled peptide was eluted with 50% ethanol.

Quality control of the radiolabeled preparations

Radiochemical purity was determined using instant thin-layer chromatography (ITLC) on silica-gel strips (Pall Life Sciences, Ann Arbor, MI) using 0.1 M citrate buffer, pH 6.0 as the mobile phase. The colloid content of the radiolabeled peptide was determined by ITLC-SG using a 1:1 v/v solution of 0.15 M NH_4Ac, pH 5.5, MeOH as the mobile phase.

^{111}In-IMP-288, ^{68}Ga-IMP-288 and ^{18}F-IMP-449 were analyzed by RP-HPLC (Agilent 1100 series, Agilent Technologies, Palo Alto, CA) on a RP C_{18} column (Alltima, 5 μm, 4.6 × 250 mm, Alltech, Deerfield, IL), using a flow rate of 1.0 ml/min with a linear gradient of 97% A and 3% to 100% B, over 15 min buffer A: 0.1 % TFA in water and buffer B: 0.1 % TFA in acetonitrile. Radiochemical purity of ^{125}I-TF2, ^{111} In- and ^{68}Ga- IMP-288 and ^{18}F-IMP-449 preparations always exceeded 95%.

Animal experiments

All studies were approved by the institutional Animal Welfare Committee of the Radboud University Medical Centre Nijmegen, and conducted in accordance with their guidelines (revised Dutch Act on Animal Experimentation, 1997). Male nude BALB/c mice (6-8 weeks old), weighing 20-25 grams, received a subcutaneous injection with 0.2 mL of a suspension of 1×10^6 LS174T, a CEA-expressing human colon carcinoma cell line (CCL-188, American Type Culture Collection, Rockville, MD, passage 7). In some studies, animals were co-implanted with SK-RC 52 cells, a human renal cancer cell line that is negative for CEA (20). The CEA production of LS174T in the ATCC seed stock was 1944 ng per milion cells in 10 days. Homogenized tissue of subcutaneous LS174T and SK-RC 52 tumors during 10 days, grown in nude BALB/c mice, showed that the LS174T tumor had a CEA content of 17745 ng per million cells, whereas the SK-RC 52 tumor had no detectable CEA content. Studies were initiated when the tumors reached a size of about 0.1-0.3 g.

In separate studies, animals bearing an LS174T xenograft in one hind leg were injected in the other hind limb muscle with 50 μl of turpentine to induce an inflammatory reaction (21).

TF2 was given intravenously and 16 hours later, radiolabeled IMP-288 was given in 0.2 mL. This interval was shown previously to be sufficient to clear TF2 from the circulation (15). In some studies, ^{125}I-TF2, (0.4 MBq) was co-injected with unlabeled TF2. One hour after the injection of ^{68}Ga-labeled peptide, and two hours after injection of ^{18}F-IMP-449, mice were euthanized by CO_2/O_2, and blood was obtained by cardiac puncture.

PET images were acquired with an Inveon animal PET/CT scanner (Siemens Preclinical Solutions, Knoxville, TN) with an intrinsic spatial resolution of 1.5 mm (22). The animals were placed in a supine position. PET emission scans were acquired for 15 min, preceded by CT scans for anatomical reference (spatial resolution 113 μm, 80 kV, 500 μA, exposure time 300 msec). Scans were reconstructed using Inveon Acquisition Workplace software (version 1.2, Siemens Preclinical Solutions, Knoxville, TN, USA) using a 3D ordered subset expectation maximization/maximum a posteriori (OSEM3D/MAP) algorithm with the following parameters: matrix 256 × 256 × 159, pixel size 0.43 × 0.43 × 0.8 mm^3 and MAP prior β of 0.5.

After imaging, tumor and organs of interest were dissected, weighed and counted in a gamma counter with appropriate energy windows for ^{125}I, ^{111}In, ^{68}Ga or ^{18}F. The percentage-injected dose per gram tissue (% ID/g) was calculated.

Statistic analysis

All mean values are given ± standard deviation (S.D.) Statistical analysis was performed using a non-parametric, two-tailed Mann Whitney test using GraphPad InStat software (version 4.00, GraphPad Software). The level of significance was set at $P<0.05$.

Results

Dose optimization

The effect of the TF2 dose on tumor targeting with a fixed amount of IMP-288 (0.01 or 0.1 nmole; 15 or 150 ng, respectively) was determined. Groups of five mice were injected intravenously with 0.10, 0.25, 0.50 or 1.0 nmol TF2, labeled with a trace amount of ^{125}I (0.4 MBq). Two hours after injection of ^{111}In-IMP-288 (0.01 nmol, 0.4 MBq), the biodistribution of the radiolabels was determined.

TF2 cleared rapidly from blood and normal tissues. Eighteen hours after injection, the blood concentration was less than 0.45% ID/g at all TF2 doses tested. TF2 tumor uptake was 3.5% ID/g, independent of TF2 dose up to 1.0 nmol (data not shown). At all TF2 doses, ^{111}In-IMP-288 accumulated effectively in the tumor, with increasing uptake associated with higher TF2 doses (Figure 2a). At the 0.01 nmole ^{111}In-IMP-288 dose, tumor uptake peaked at 26.2 ± 3.8% ID/g. With 0.01 nmol of IMP-288, the highest tumor targeting and tumor-to-blood ratios were achieved with 1.0 nmol TF2 (TF2:IMP-288 molar ratio = 100:1). The kidneys had the highest normal organ accretion of ^{111}In-IMP-288 (1.75 ± 0.27% ID/g); all other normal tissues had very low uptake.

With ^{68}Ga-labeled IMP-288, a minimum of 5-10 MBq ^{68}Ga was required for PET imaging performed 1 h after injection. At a maximum specific activity of 50-125 MBq/nmol at the time of injection, at least 0.1-0.25 nmol of ^{68}Ga-IMP-288 had to be administered. A separate group of LS174T-bearing mice received the same TF2:IMP-288 molar ratios as were tested above, but with 0.1 nmol IMP-288, 1.0, 2.5, 5.0 or 10.0 nmol of TF2 was administered. The percent uptake of TF2 in the tumor decreased from 3.21 ± 0.61% ID/g at the 1.0 nmole dose to 1.16 ± 0.27% ID/g with 10.0 nmol, suggesting the antigen in the tumor was saturated. In contrast to the results at the 0.01 nmole dose, tumor uptake with 0.1 nmole of ^{111}In-IMP-288 was not affected by the TF2 dose, but it did not exceed about 15% ID/g at all doses tested (Figure 2b). Based on these data, a bsMAb dose of 6.0 nmol was selected for targeting 0.1-0.25 nmol of ^{68}Ga-IMP-288 to the tumor.

PET imaging

Five mice bearing an LS174T CEA-expressing tumor in the right flank and SK-RC 52, a CEA-negative tumor in the left flank were administered 6.0 nmol ^{125}I-TF2 intravenously. After 16 h, the mice received 5 MBq ^{68}Ga-IMP-288 (0.25 nmol, specific activity of 20 MBq/nmol). A separate group of three mice received the same amount of ^{68}Ga-IMP-288 alone, without pretargeting with TF2. PET/CT scans of the mice were acquired 1 h after injection of the ^{68}Ga-IMP-288.

The biodistribution of ^{125}I-TF2 and ^{68}Ga-IMP-288 in mice are shown in Figure 3a. High uptake of the bsMAb (2.17 ± 0.50% ID/g) and peptide (10.7 ± 3.6% ID/g) in the tumor was observed, with very low accretion in the normal tissues (tumor-to-blood ratio for ^{68}Ga-IMP-288: 64 ± 22). Most importantly, targeting of ^{68}Ga-IMP-288 in the CEA-negative tumor SK-RC 52 was very low (0.35 ± 0.35% ID/g). Likewise, tumors that were not pretargeted with TF2 had a low uptake of ^{68}Ga-IMP-288 (0.20 ± 0.03% ID/g), indicating that the specific accumulation of IMP-288 in the CEA-expressing LS174T tumor was derived from the pre-localization of the bsMAb.

The specific uptake of ^{68}Ga-IMP-288 in the CEA-expressing tumor pretargeted with TF2 was clearly visualized in the PET image acquired 1 h after injection, without any localization in the negative tumor (Figure 3b). Uptake in the tumor was evaluated quantitatively by drawing regions of interest (ROI), using a 50% threshold of maximum intensity. A region in the abdomen was used as background region. The tumor-to-background ratio in the image of the mouse that received TF2 and ^{68}Ga-IMP-288 was 38.2 at 1 h.

In the next studies, two groups of five mice bearing a s.c. LS174T tumor in the right hind leg and an turpentine-induced inflammatory focus in the left thigh muscle were examined to assess the specificity of the pretargeting procedure compared to ^{18}F-FDG. Three days after the induction of the inflammatory lesion, one group of mice received 6.0 nmol TF2, followed 16 h later by 5 MBq ^{68}Ga-IMP-288 (0.25 nmol). The other group received ^{18}F-FDG (5 MBq). Mice were fasted for 10 hours prior to the injection and anesthetized and kept warm at 37 °C until euthanasia, 1 h post-injection.

Figure 4a shows an example of a mouse that received the TF2-pretargeted ^{68}Ga-IMP-288, showing efficient accretion of the radiolabeled peptide in the tumor, while the inflamed muscle was not visualized. In contrast, both tumor and inflammation were visible in the mice that received ^{18}F-FDG (Figure 4b). In mice given ^{68}Ga-IMP-288, the tumor-to-inflamed tissue ratio by SUV analysis was 5.4 and the tumor-to-background ratio was 48. ^{18}F-FDG uptake had a tumor-to-inflamed muscle ratio of 0.83, and the tumor-to-background ratio was 2.4.

At necropsy, uptake of ^{68}Ga-IMP-288 measured in the inflamed muscle was only 0.72 ± 0.20% ID/g, but tumor uptake was 8.73 ± 1.60% ID/g (P<0.05, Figure 5). The tumor-to-blood ratio of ^{68}Ga-IMP-288 in these mice was 69.9 ± 32.3; the inflamed muscle-to-blood ratio was 5.9 ± 2.9; and the tumor-to-inflamed muscle ratio was 12.5 ± 2.1. ^{18}F-FDG accreted efficiently in the tumor (7.42 ± 0.20% ID/g, tumor-to-blood ratio 6.24 ± 1.5, Figure 5), but also accumulated substantially in the inflamed muscle (4.07 ± 1.13% ID/g), with an inflamed muscle-to-blood ratio of 3.4 ± 0.5, and a tumor-to-inflamed muscle ratio of 1.97 ± 0.71.

Finally, the pretargeted immunoPET imaging method was tested using the ^{18}F-labeled peptide, IMP-449. Five mice received 6.0 nmol TF2, followed 16 h later by 5 MBq ^{18}F-IMP-449 (0.25 nmol). Three additional mice received 5 MBq ^{18}F-IMP-449 without prior administration of TF2, while two mice were injected with Al[^{18}F]$^{2+}$ (3 MBq). Uptake of ^{18}F-IMP-449 at 1 h in tumors pretargeted with TF2 was high (10.6 ± 1.7% ID/g) (Figure 6), whereas it was very low in the non-pretargeted mice (0.45 ± 0.38 % ID/g). Al[^{18}F]$^{2+}$ accumulated in the bone (50.9 ± 11.4% ID/g), while uptake of IMP-449 peptide in the bone was very low (0.54 ± 0.2% ID/g), indicating that the ^{18}F-IMP-449 was stable *in vivo*. Importantly, the biodistribution of ^{18}F-IMP-449 in the TF2 pretargeted mice was very similar to that of ^{68}Ga-IMP-288, indicating the suitability for either of these radiolabeled agents for use in pretargeted PET imaging. Pretargeted immunoPET images with ^{18}F-IMP-449 showed the same intensity in the tumor as those with ^{68}Ga-IMP-288, but the resolution of the ^{18}F-images was better than the ^{68}Ga-images (Figure 7). The tumor-to-background ratio of the ^{18}F-IMP-449 signal was 66.

Discussion

Several important conclusions can be made from the present study. Pretargeting affords the possibilities of utilizing antibody-based imaging techniques with short-lived radionuclides, such as ^{68}Ga and ^{18}F, that are ideally suited for PET imaging. Before the use of ^{18}F-FDG and PET imaging, radiolabeled antibodies were being developed commercially for the detection of colorectal, ovarian, lung, and prostate cancers using single-photo computed emission tomography imaging systems (23). However, all of these imaging methods suffered from relatively poor contrast, even when radiolabeled antibody fragments were used (24).

Unquestionably, the advent of ^{18}F-FDG provided the necessary platform for the development of molecular imaging based on the newly developed PET imaging systems, and as a result, most of these antibody-imaging agents have been withdrawn from the market. Since then, molecular engineering has fostered a new era for antibodies, making it possible to craft many different forms with more favorable blood clearance and targeting potential (25). Still, many of these new constructs require considerable time for good tumor uptake and contrast to develop, and therefore radionuclides with longer half-lives, such as ^{64}Cu and ^{124}I, are often used. For example, Cai et al. reported an attempt to use a directly radiolabeled ^{18}F-anti-CEA diabody for imaging (26). While this type of construct has very favorable pharmacokinetic properties, maximum tumor uptake in LS174T xenografts obtained at 1 h post- injection was only 2.7% ID/g, along with 2.0% ID/g in the blood and higher uptake in the other major organs. Low, but favorable tumor/tissue ratios required 4-6 h to develop. ^{124}I has been used with directly radiolabeled antibody constructs for a large part because radioiodine will not be retained in normal tissues, and thus more reasonable tumor/tissue ratios can be achieved than with a radiometal (27). However, the added expense and relatively poor imaging properties of this radionuclide are considerable barriers to the development of products based on ^{124}I. As our studies show, the short physical half-life of ^{18}F and ^{68}Ga can be used effectively in pretargeting to enhance detection sensitivity.

The half-life of ^{68}Ga is well matched to the kinetics of the IMP-288 peptide in the pretargeting system. ^{68}Ga can be eluted twice daily from a ^{68}Ge/^{68}Ga generator, avoiding the need for an on-site cyclotron. However, the high energy of the positrons emitted by ^{68}Ga (1.9 MeV) limits the spatial resolution of the acquired images to 3 mm, while the intrinsic resolution of the microPET system is as low as 1.5 mm (22). In the clinical setting, the penetration range of ^{68}Ga positrons does not reduce the resolution of the images. For these studies, the procedure to label IMP-288 with ^{68}Ga was optimized, resulting in a one-step labeling technique. We found that purification on a C18/HLB cartridge was required to remove the ^{68}Ga colloid that is inevitably formed when the peptide was labeled at specific activities exceeding 150 GBq/nmol at 95 °C. ^{68}Ga colloid accumulates in tissues of the reticuloendothelial system (liver, spleen, and bone marrow), deteriorating image quality, but it could be effectively reduced by rapid purification on a C18-cartridge. Radiolabeling and purification for administration could be accomplished within 45 minutes.

^{18}F, the most widely used radionuclide in PET, has an even more favorable half-life for pretargeted PET imaging (t½ = 110 min). Therefore, in this study, the NOTA-conjugated peptide, IMP-449, was labeled with ^{18}F, as recently described by McBride et al. (13). We showed that this method produces a preparation that is stable *in vivo*. Similar to labeling with ^{68}Ga, it is a one-step procedure, which currently requires HPLC purification to remove the unlabeled peptide to enhance specific activity. Labeling yield was as high as 50%. Interestingly, the biodistribution of ^{18}F-IMP-449 was similar to that of ^{68}Ga-labeled IMP-288, suggesting that the new labeling method using NOTA to chelate Al[^{18}F]$^{2+}$ turns the ^{18}F-label into a residualizing radionuclide. Presumably, the peptide undergoes proteolytic degradation in the lysosomes and its radiolabeled catabolite, containing Al[^{18}F]$^{2+}$-NOTA, is trapped in the lysosomes, as has been described for radiometals.

In contrast to FDG-PET, pretargeted radioimmunodetection is a tumor-specific imaging modality. Although a high sensitivity and specificity for FDG-PET in detecting recurrent colorectal cancer lesions has been reported in patients (28), FDG-PET images could lead to diagnostic dilemmas in discriminating malignant from benign, highly metabolic lesions, such as inflammation. Earlier studies in animal models have highlighted the improvements that an antibody-based pretargeting procedure can provide in comparison to ^{18}F-FDG, focusing primarily on its enhanced sensitivity (12). In this study, we addressed the specificity of pretargeting in relation to its ability to discriminate inflammatory lesions from cancer. As

expected, ^{18}F-FDG had high uptake in the tumor, but this was only 2-fold higher than the uptake in the inflammatory lesion. In contrast, tumor uptake was at least 10-fold higher in the tumor as compared to the inflammatory lesion with the antibody-based pretargeting method. Additionally, we showed that pretargeting specifically localizes in the intended target, with a 30-times higher concentration in the antigen-positive tumor than in a negative tumor. Thus, with evidence for appreciable improvements in both sensitivity and specificity, bsMAb-based pretargeting procedures could provide important new tools for detecting cancer.

This pretargeting method is a 2-step process that first requires the administration of the unlabeled bsMAb. Rather than using a clearing agent, the bsMAb are designed in a manner to minimize their residence time in the blood. Despite its size equaling that of an IgG (i.e., 157 kD), TF2 is cleared very quickly. The long circulatory half-life of IgG is only partly determined by its large size, and is mainly due to the presence of the C_H2 domain, which enables recycling via FcRn-receptors (29). It has been shown that C_H2 domain-deleted variants of IgG (121 kDa) clear much faster from the blood than intact IgG (30,31). TF2 is an engineered trivalent antibody derived from three Fab-fragments and lacks any C_H2 domain.

These studies also provide new insights into this pretargeting method. Earlier studies examined the effects of increasing the bsMAb with a fixed amount of the peptide in mice with GW-39 human colonic tumors. It was reported that beyond a 10:1 molar ratio of bsMAb:peptide, the amount of peptide that could be delivered to the tumor did not increase (32). Using a low peptide dose level (0.01 nmol), we found tumor uptake in the LS174T model increased as the moles of bsMAb were increased from 0.1 to 1 nmole, reaching a maximum uptake of ~25% ID/g with 1 nmole of TF2 (i.e., a 100:1 mole ratio) with minimal changes in blood and normal tissue uptake.

Compared to earlier studies, a number of factors contributed to the need for injecting considerably more hapten-peptide in these studies, including the size and age of the ^{68}Ga-generator, yields after purification, and the natural decay of the product that required a minimum of 5 MBq to be administered for imaging. Thus, a separate biodistribution study was performed to examine a similar dose-response with 10-fold more IMP-288 (0.1 nmole). Despite administering increasing amounts of TF2 at the same mole ratios used with 0.01 nmole of IMP-288, tumor uptake remained highly favorable, but remained at a constant level of ~15% ID/g over a TF2 dose range of 1 to 10 nmoles. TF2 tumor uptake showed a constant level of ~3% ID/g over a dose range from 0.1 to 1.0 nmol, but at the 2.5 nmol dose the percent uptake began to decline, reducing to ~1% ID/g at 10 nmole. As a result, at the high IMP288 dose (0.1 nmol), increasing the TF2 dose did not result in higher tumor uptake of radiolabeled IMP288. These data suggest that at TF2 doses exceeding 2.5 nmol, saturation of CEA in the tumor (with TF2) occurs. Thus, in pretargeting, exceptionally favorable targeting at lower specific activities can be achieved, but a higher fractional uptake results at its highest specific activity.

In conclusion, pretargeted immunoPET with an anti-CEA bsMAb and a ^{68}Ga- or ^{18}F-hapten-peptide is a rapid, highly specific and sensitive imaging modality for the detection CEA-positive tumors.

Acknowledgments

Grant support: Dutch Cancer Society (KWF Kankerbestrijding) grant no. KUN 2008-4038, and NIH grant 1 R43 EB003751 from the National Institute of Biomedical Imaging and Bioengineering.

Reference List

1. Jain RK. Physiological barriers to delivery of monoclonal antibodies and other macromolecules in tumors. Cancer Res 1990;50:814s–9s. [PubMed: 2404582]

2. Sharkey RM, Karacay H, Cardillo TM, et al. Improving the delivery of radionuclides for imaging and therapy of cancer using pretargeting methods. Clin Cancer Res 2005;11:7109s–21s. [PubMed: 16203810]
3. Reardan DT, Meares CF, Goodwin DA, et al. Antibodies against metal chelates. Nature 1985;316:265–8. [PubMed: 3927170]
4. Boerman OC, van Schaijk FG, Oyen WJ, Corstens FH. Pretargeted radioimmunotherapy of cancer: progress step by step. J Nucl Med 2003;44:400–11. [PubMed: 12621007]
5. Chang CH, Sharkey RM, Rossi EA, et al. Molecular advances in pretargeting radioimunotherapy with bispecific antibodies. Mol Cancer Ther 2002;1:553–63. [PubMed: 12479274]
6. Sharkey RM, Cardillo TM, Rossi EA, et al. Signal amplification in molecular imaging by pretargeting a multivalent, bispecific antibody. Nat Med 2005;11:1250–5. [PubMed: 16258537]
7. Le Doussal JM, Martin M, Gautherot E, Delaage M, Barbet J. In vitro and in vivo targeting of radiolabeled monovalent and divalent haptens with dual specificity monoclonal antibody conjugates: enhanced divalent hapten affinity for cell-bound antibody conjugate. J Nucl Med 1989;30:1358–66. [PubMed: 2787847]
8. Karacay H, McBride WJ, Griffiths GL, et al. Experimental pretargeting studies of cancer with a humanized anti-CEA × murine anti-[In-DTPA] bispecific antibody construct and a (99m)Tc-/(188) Re-labeled peptide. Bioconjug Chem 2000;11:842–54. [PubMed: 11087333]
9. Griffiths GL, Chang CH, McBride WJ, et al. Reagents and methods for PET using bispecific antibody pretargeting and 68Ga-radiolabeled bivalent hapten-peptide-chelate conjugates. J Nucl Med 2004;45:30–9. [PubMed: 14734668]
10. McBride WJ, Zanzonico P, Sharkey RM, et al. Bispecific antibody pretargeting PET (immunoPET) with an 124I-labeled hapten-peptide. J Nucl Med 2006;47:1678–88. [PubMed: 17015905]
11. Sharkey RM, McBride WJ, Karacay H, et al. A universal pretargeting system for cancer detection and therapy using bispecific antibody. Cancer Res 2003;63:354–63. [PubMed: 12543788]
12. Sharkey RM, Karacay H, Vallabhajosula S, et al. Metastatic human colonic carcinoma: molecular imaging with pretargeted SPECT and PET in a mouse model. Radiology 2008;246:497–507. [PubMed: 18227543]
13. McBride WJ, Sharkey RM, Karacay H, et al. A novel method of 18F radiolabeling for PET. J Nucl Med 2009;50:991–8. [PubMed: 19443594]
14. Morel A, Darmon M, Delaage M. Recognition of imidazole and histamine derivatives by monoclonal antibodies. Mol Immunol 1990;27:995–1000. [PubMed: 2233759]
15. Sharkey RM, Goldenberg DM, Goldenberg H, et al. Murine monoclonal antibodies against carcinoembryonic antigen: immunological, pharmacokinetic, and targeting properties in humans. Cancer Res 1990;50:2823–31. [PubMed: 2328505]
16. Goldenberg DM, Rossi EA, Sharkey RM, McBride WJ, Chang CH. Multifunctional antibodies by the Dock-and-Lock method for improved cancer imaging and therapy by pretargeting. J Nucl Med 2008;49:158–63. [PubMed: 18077530]
17. Rossi EA, Goldenberg DM, Cardillo TM, McBride WJ, Sharkey RM, Chang CH. Stably tethered multifunctional structures of defined composition made by the dock and lock method for use in cancer targeting. Proc Natl Acad Sci U S A 2006;103:6841–6. [PubMed: 16636283]
18. Lindmo T, Boven E, Cuttitta F, Fedorko J, Bunn PA Jr. Determination of the immunoreactive fraction of radiolabeled monoclonal antibodies by linear extrapolation to binding at infinite antigen excess. J Immunol Methods 1984;72:77–89. [PubMed: 6086763]
19. Fraker PJ, Speck JC Jr. Protein and cell membrane iodinations with a sparingly soluble chloroamide, 1,3,4,6-tetrachloro-3a,6a-diphrenylglycoluril. Biochem Biophys Res Commun 1978;80:849–57. [PubMed: 637870]
20. Ebert T, Bander NH, Finstad CL, Ramsawak RD, Old LJ. Establishment and characterization of human renal cancer and normal kidney cell lines. Cancer Res 1990;50:5531–6. [PubMed: 2386958]
21. Van der Laken CJ, Boerman OC, Oyen WJ, et al. In vivo expression of interleukin-1 receptors during various experimentally induced inflammatory conditions. J Infect Dis 1998;177:1398–401. [PubMed: 9593033]
22. Visser EP, Disselhorst JA, Brom M, et al. Spatial resolution and sensitivity of the Inveon small-animal PET scanner. J Nucl Med 2009;50:139–47. [PubMed: 19139188]

23. Van de Wiele C, Revets H, Mertens N. Radioimmunoimaging. Advances and prospects. Q J Nucl Mol Imaging 2004;48:317–25.
24. Goldenberg DM. Perspectives on oncologic imaging with radiolabeled antibodies. Cancer 1997;80:2431–5. [PubMed: 9406694]
25. Wu AM, Olafsen T. Antibodies for molecular imaging of cancer. Cancer J 2008;14:191–7. [PubMed: 18536559]
26. Cai W, Olafsen T, Zhang X, et al. PET imaging of colorectal cancer in xenograft-bearing mice by use of an 18F-labeled T84.66 anti-carcinoembryonic antigen diabody. J Nucl Med 2007;48:304–10. [PubMed: 17268029]
27. Sharkey RM, Motta-Hennessy C, Pawlyk D, Siegel JA, Goldenberg DM. Biodistribution and radiation dose estimates for yttrium- and iodine-labeled monoclonal antibody IgG and fragments in nude mice bearing human colonic tumor xenografts. Cancer Res 1990;50:2330–6. [PubMed: 2180566]
28. Huebner RH, Park KC, Shepherd JE, et al. A meta-analysis of the literature for whole-body FDG PET detection of recurrent colorectal cancer. J Nucl Med 2000;41:1177–89. [PubMed: 10914907]
29. Ghetie V, Ward ES. FcRn: the MHC class-I-related receptor that is more than an IgG transporter. Immunol Today 1997;18:592–598. [PubMed: 9425738]
30. Chinn PC, Morena RA, Santoro DA, et al. Pharmacokinetics and tumor localization of (111)In-labeled HuCC49DeltaC(H)2 in BALB/c mice and athymic murine colon carcinoma xenograft. Cancer Biother Radiopharm 2006;21:106–116. [PubMed: 16706631]
31. Slavin-Chiorini DC, Kashmiri SV, Lee HS, et al. A CDR-grafted (humanized) domain-deleted antitumor antibody. Cancer Biother Radiopharm 1997;12:305–316. [PubMed: 10851481]
32. Sharkey RM, Karacay H, Richel H, et al. Optimizing bispecific antibody pretargeting for use in radioimmunotherapy. Clin Cancer Res 2003;9:3897S–913S. [PubMed: 14506188]

Abbreviations list

bsMAb	bispecific monoclonal antibody
BSA	bovine serum albumin
CEA	Carcinoembryonic antigen
EDTA	ethylenediaminetetraacetic acid
FDG	Fluorodeoxyglucose
HSG	histamine-succinyl-glycine
ITLC	Instant thin-layer chromatography
RP-HPLC	reversed phase-high performance liquid chromatography

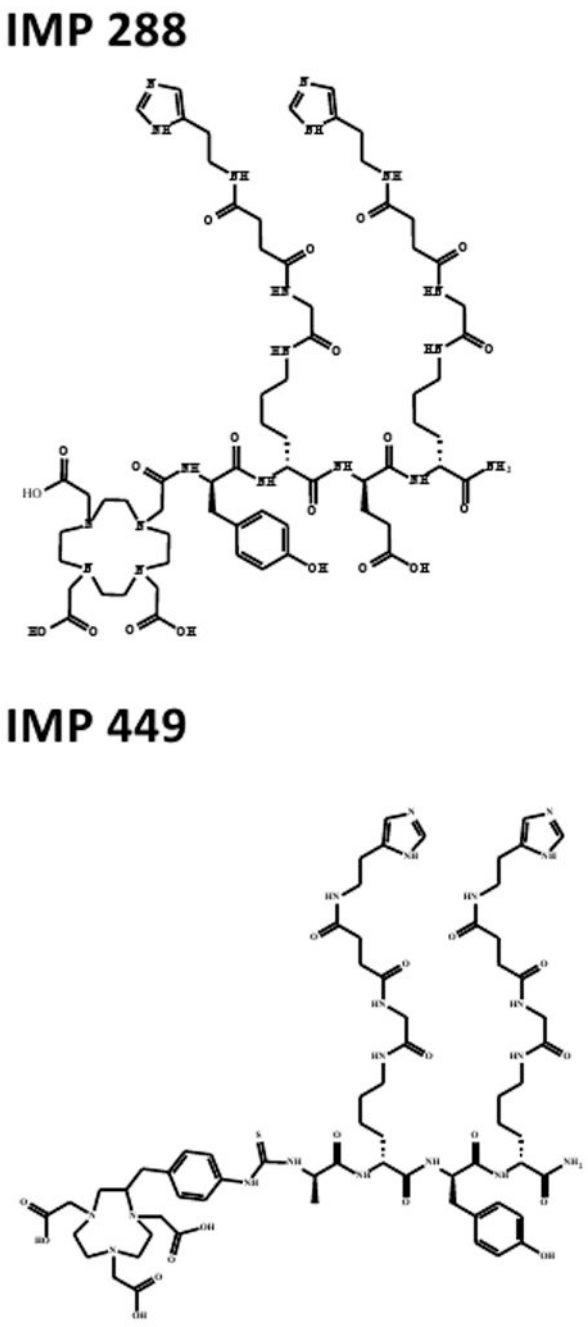

Figure 1.
Chemical structures of IMP288 and IMP449. Both are Tyr-D-Lys-D-Glu-D-Lys tetrapeptides in which both lysine residues are substituted with a HSG-moiety via their ε-aminogroup. IMP288 is conjugated with DOTA: 7,10-tetra-azacyclododecane-N,N′,N″,N‴-tetraacetic acid and IMP-449 is conjugated with NOTA: 1,4,7-tri-azacyclononane-N,N′,N″-triacetic acid.

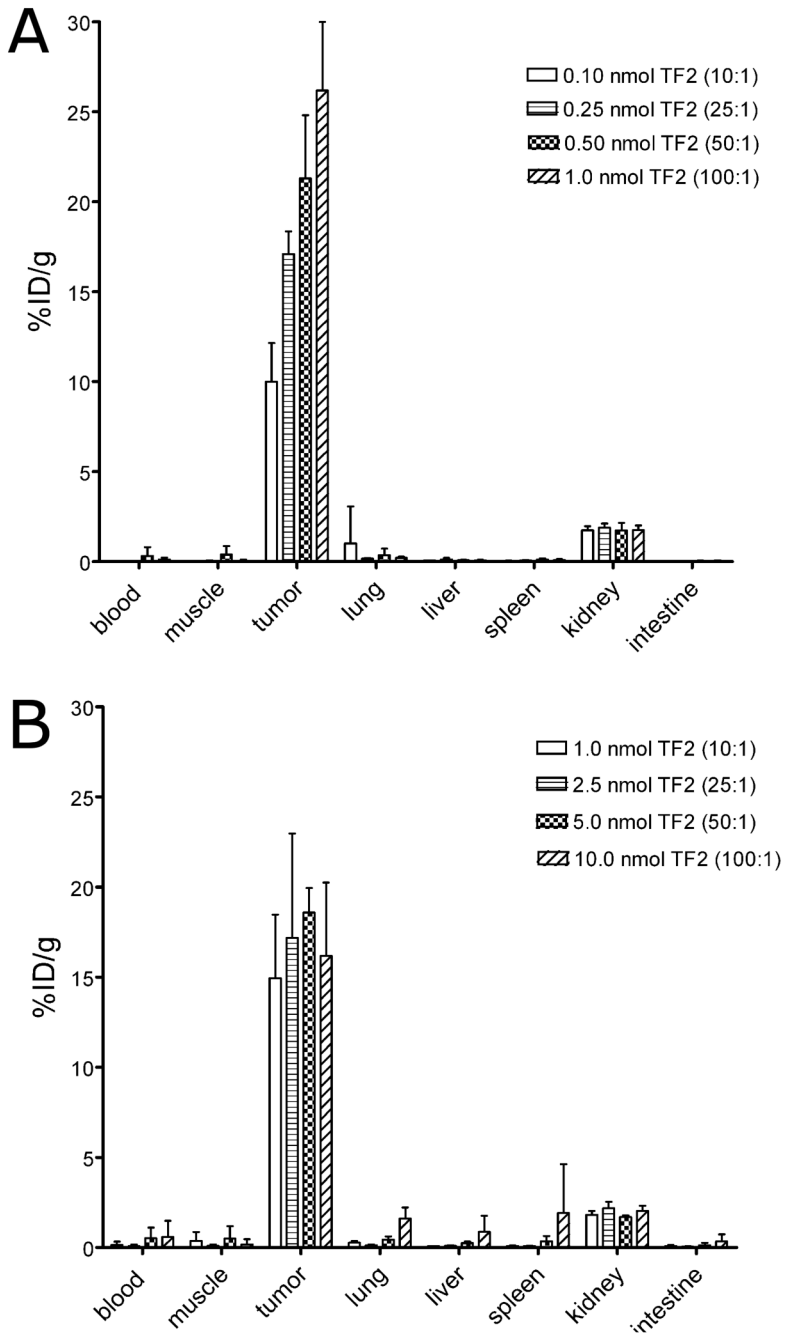

Figure 2.

Biodistribution of ^{111}In-IMP-288 1 h after i.v. injection, following pretargeting with escalating doses TF2 in BALB/c nude mice with a s.c. CEA-expressing LS174T tumor. Two peptide doses were tested (1A. 0.01 nmol ^{111}In-IMP-288; 1B. 0.10 nmol ^{111}In-IMP-288). Values are given as means ± standard deviation (n=5).

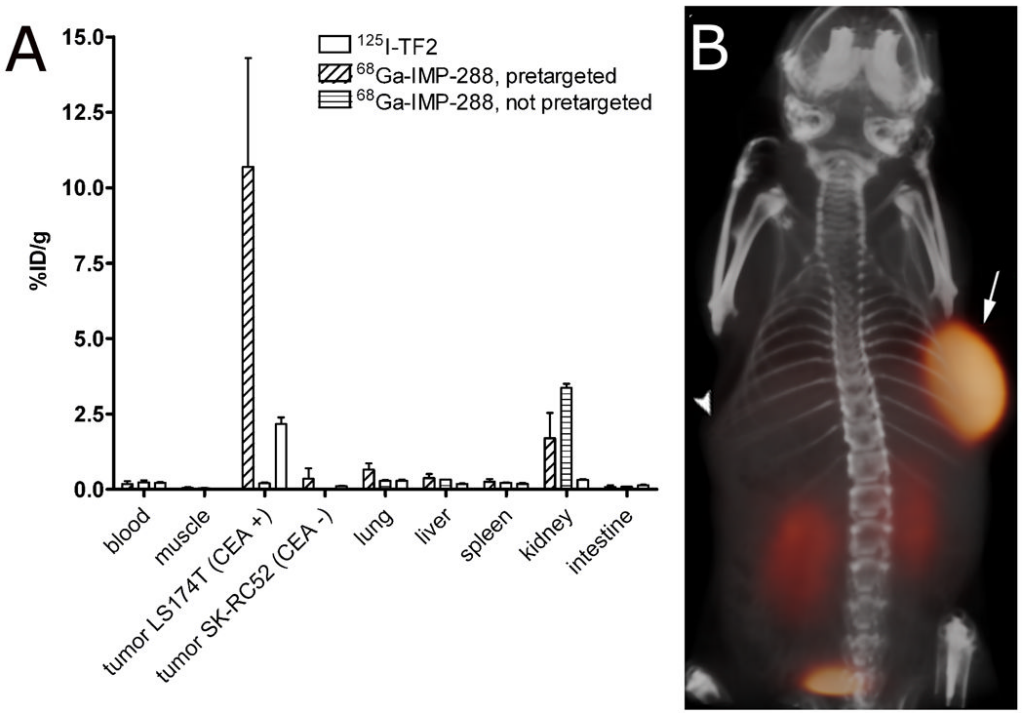

Figure 3.

Biodistribution of 6.0 nmol ^{125}I-TF2 (0.37 MBq) and 0.25 nmol ^{68}Ga-IMP-288 (5 MBq), 1 h after i.v. injection of ^{68}Ga-IMP-288 in BALB/c nude mice with a subcutaneous LS174T and SK-RC52 tumor. Values are given as means ± standard deviation (n=5) (A). 3D volume rendering of PET/CT image of a BALB/c nude mouse with a subcutaneous LS174T CEA-expressing tumor in the right flank (arrow) and a subcutaneous SK-RC 52 tumor, a non-CEA-producing, tumor in the left flank (arrowhead), that received 6.0 nmol TF2 and 5 MBq ^{68}Ga-IMP-288 (0.25 nmol) intravenously with a 16-hour interval, imaged one hour after ^{68}Ga-IMP-288 injection (B).

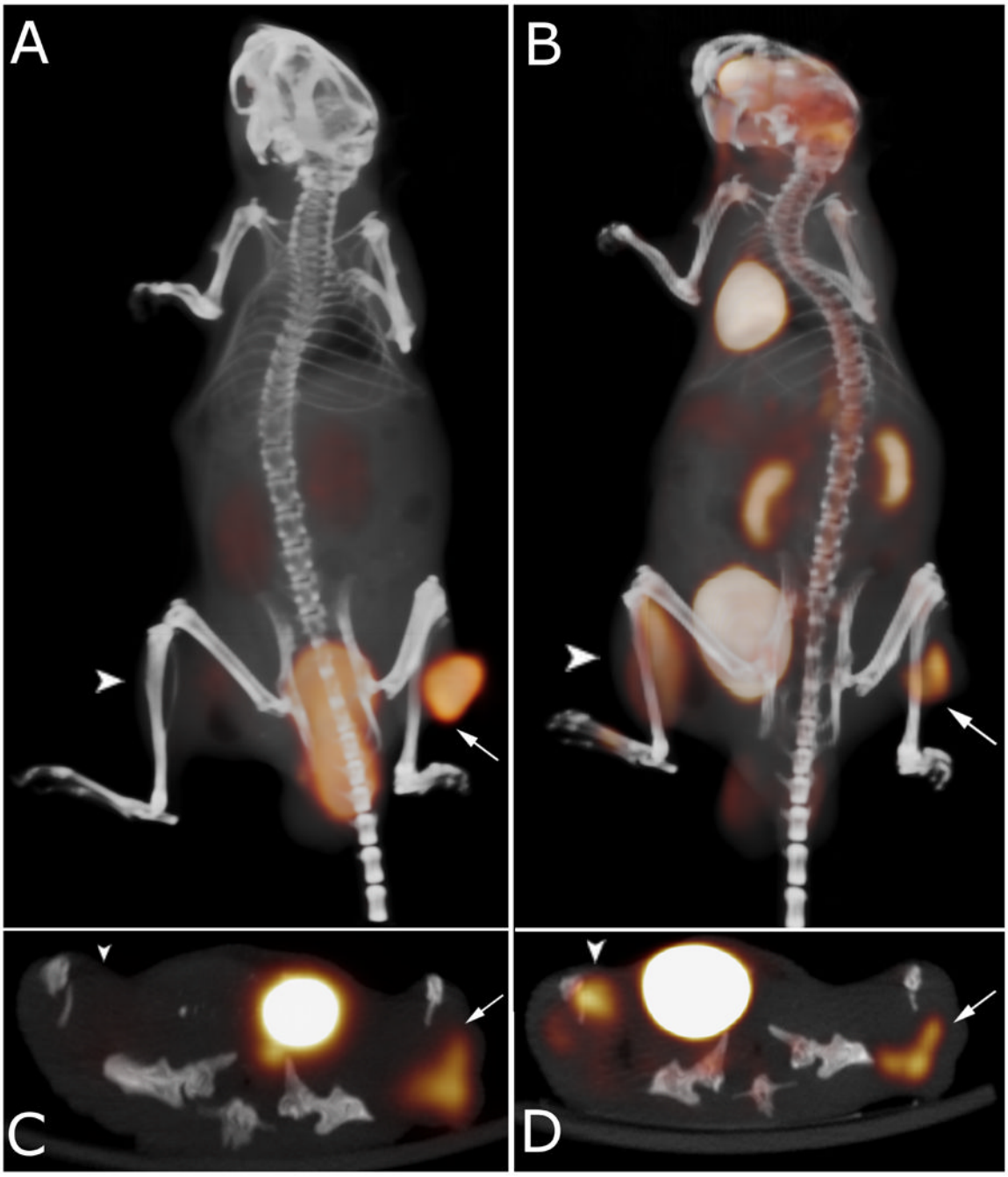

Figure 4.
PET/CT images of a BALB/c nude mouse with a subcutaneous LS174T tumor (0.1 g) on the right hind leg (arrow) and a inflammation in the left thigh muscle (arrowhead), that received 5 MBq ^{18}F-FDG, and one day later 6.0 nmol TF2 and 5 MBq ^{68}Ga-IMP-288 (0.25 nmol) with a 16-hour interval. The animal was imaged one hour after ^{18}F-FDG and ^{68}Ga-IMP-288 injections. The panel shows the 3D volume rendering of the pretargeted immunoPET scan (A) and of the FDG-PET scan (B), and the transverse sections of the tumor region of the pretargeted immunoPET scan (C), and of the FDG-PET scan (D).

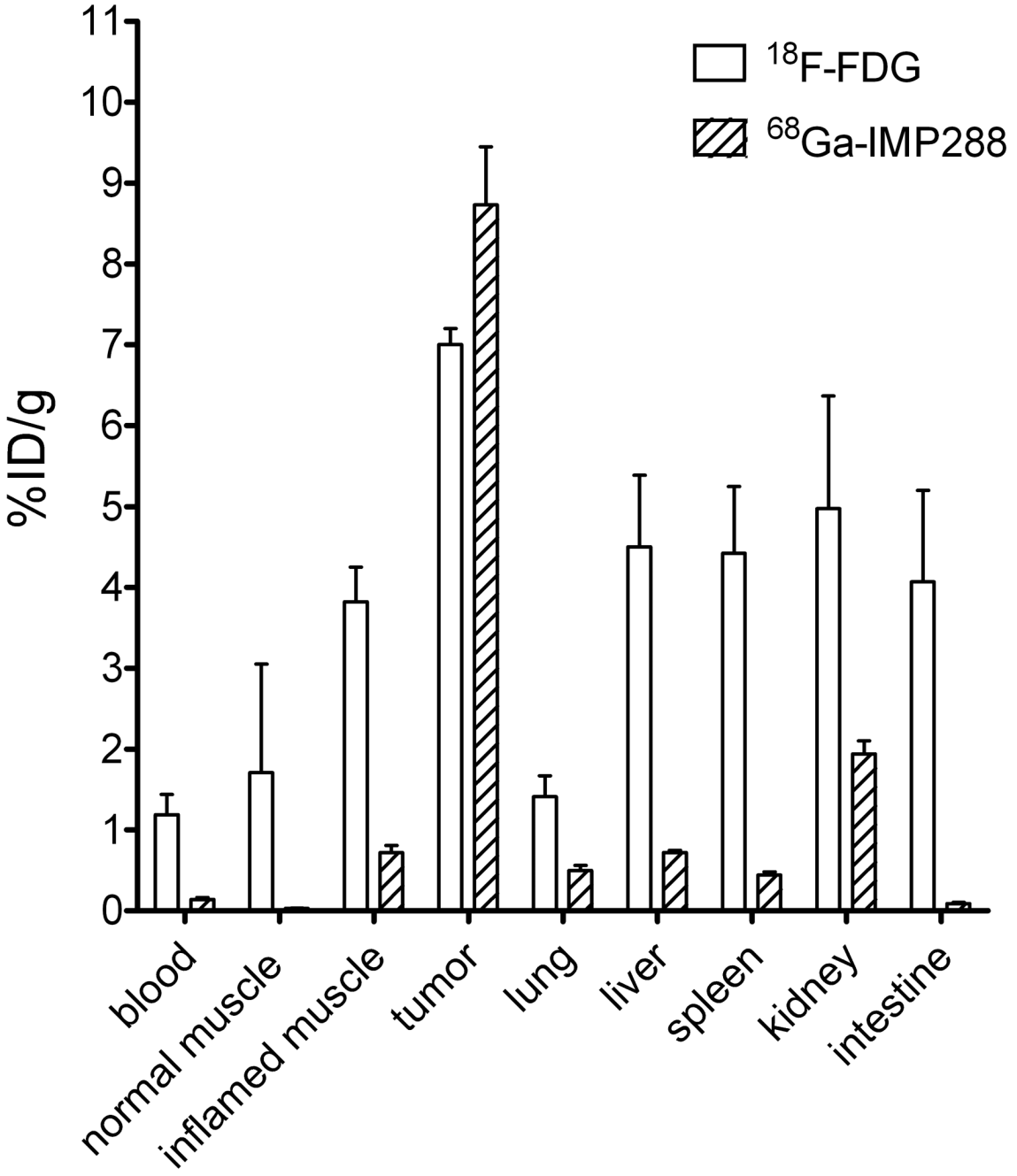

Figure 5.
Biodistribution of 5 MBq FDG and 5 MBq ^{68}Ga-IMP-288 (0.25 nmol) 1 h after injection, following pretargeting with 6.0 nmol TF2 in BALB/c nude mice with a s.c. CEA-expressing LS174T tumor. Values are given as means ± standard deviation (n=5).

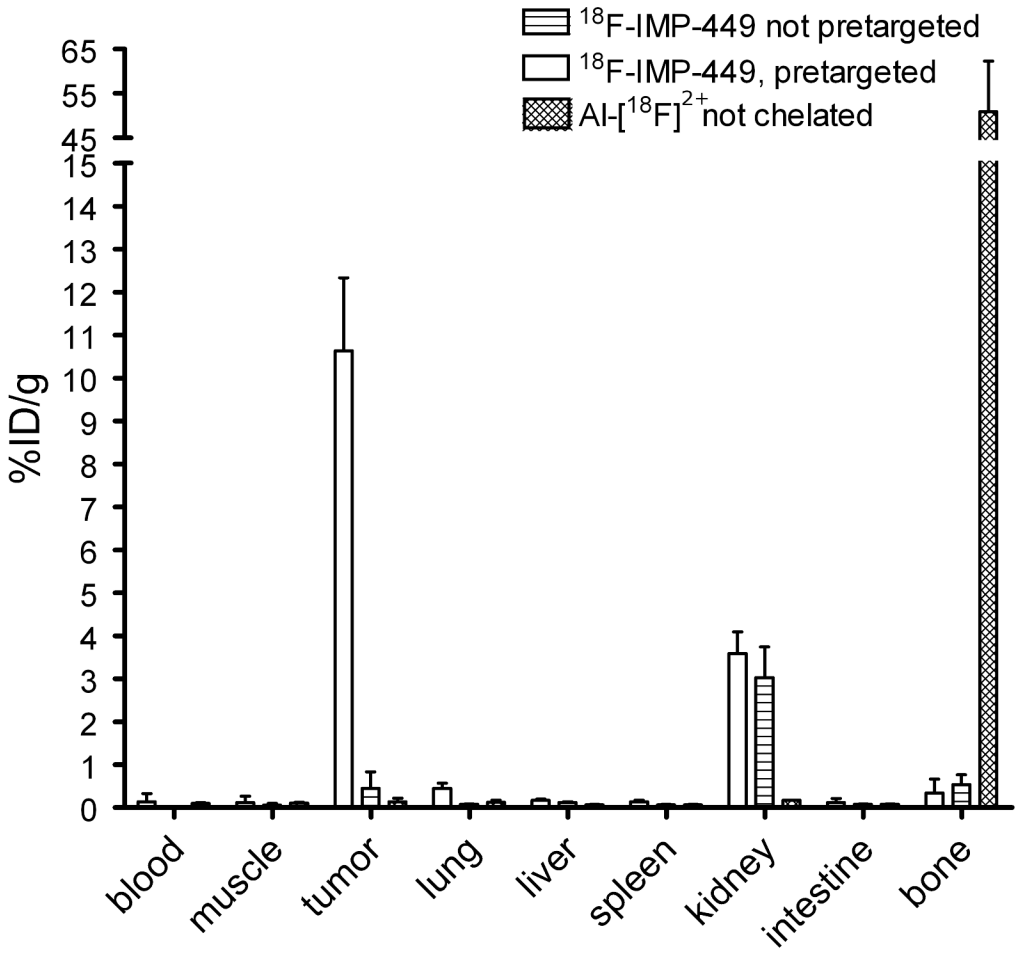

Figure 6.

Biodistribution of 0.25 nmol ^{18}F-IMP-449 (5 MBq) 1 hour after injection, following pretargeting with 6.0 nmol TF2 16 hours earlier, biodistribution of ^{18}F-IMP-449 without pretargeting, or biodistribution of Al[^{18}F]$^{2+}$ in BALB/c nude mice with a s.c. CEA-expressing LS174T tumor. Values are given as means ± standard deviation.

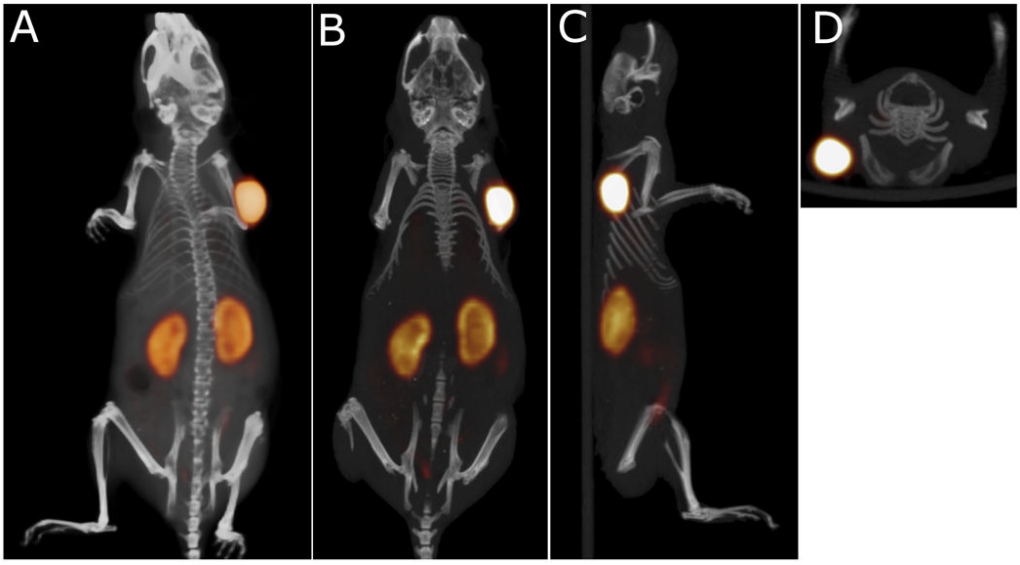

Figure 7.

Static PET/CT imaging study of a BALB/c nude mouse with a subcutaneous LS174T tumor (0.1 g) on the right side, that received 6.0 nmol TF2 and 0.25 nmol ^{18}F-IMP-449 (5 MBq) intravenously with a 16-hour interval. The animal was imaged one hour after injection of ^{18}F-IMP-449. The panel shows the 3D volume rendering (A: posterior view), and cross-sections at the tumor region (B: coronal, C: sagittal, D: transversal).